Int. J. Nonlinear Anal. Appl. 14 (2023) 5, 169–176
ISSN: 2008-6822 (electronic)
http://dx.doi.org/10.22075/ijnaa.2021.25014.2884

Methodology for modeling the information signal generator at the physical level in FANET networks

G.S. Vasilyev[a,*], O.R. Kuzichkin[a], D.I. Surzhik[a,b], I.A. Kurilov[b]

[a]Belgorod State Research University, Belgorod, 308015, Russia

[b]Vladimir State University named after Alexander Grigoryevich and Nikolai Grigorievich Stoletovs, Vladimir, 600000, Russia

(Communicated by Seyed Hossein Siadati)

Abstract

Effective design of flying ad-hoc networks (FANET) requires creating a reliable model of network behavior at various interconnection levels. The greatest differences between ad-hoc and hierarchical networks are concentrated on the lower four levels (physical, channel, network, and transport). Software simulators of computer networks have a simplified nature of the physical layer and also do not allow obtaining analytical solutions as a result of the modeling process. The developed hierarchical model for the formation of information signals allows to perform an analytical description of various communication channels and telecommunications equipment. The model can represent communication channels in a flying network while taking into account attenuation, inter-symbol interference, signal propagation over many paths, telecommunications equipment circuits with linear and nonlinear signal generation; circuits with different directions of control signals, namely direct control (FC), backward control (BC) and combined control; multi-channel circuits. Analytical transfer functions of the model are obtained for any number of unfolded hierarchy levels. The UAV transmitter frequency synthesizer is modeled on the basis of a hierarchical signal generation model. The simulation allowed us to determine the conditions for the uniformity of the amplitude-frequency modulation characteristic (AFMC) in the region of the lower modulating frequencies of the synthesizer while maintaining the high operating speed of the synthesizer.

Keywords: Unmanned aerial vehicles, FANET, Physical level, Hierarchical model, Frequency Synthesizer, Phase-locked loop
2020 MSC: 70G10

1 Introduction

Solving various tasks based on unmanned aerial vehicles (UAVs) requires the use of mobile ad-hoc networks in general (MANET) and flying ad-hoc networks (FANET) in particular. Such tasks are, in particular, the organization of security [2], signal retransmission between ad-hoc networks [3,4], monitoring of the natural environment [5,6] and technical facilities [7,8], etc.

Effective design of FANET networks requires first creating a reliable model of network behavior at various levels of OSI interaction. The most important differences between ad-hoc and hierarchical networks are concentrated on

*Corresponding author
Email addresses: vasilyevg.s@gmail.com (G.S. Vasilyev), kuzichkino.r@gmail.com (O.R. Kuzichkin), surzhik.d.i@gmail.com (D.I. Surzhik), kurilov.i.a@gmail.com (I.A. Kurilov)

Received: August 2021 *Accepted:* October 2021

the lower four levels (physical, channel, network, and transport). The problem of specialized program networking simulators, such as OPNET, ns-2/3, GNS3**,** OMNeT, is the simplified nature of the physical layer [9]. At this level, the models of radio wave propagation [10-14] and antennas [15-18] are taken into account. The influence of diverse heterogeneous factors (conditions of the ambient media, signal reflection conditions, various noises, etc.) prevents simple creation of reliable network interaction models in the FANET at the physical level. Extremely high node mobility further exacerbates the modeling problem [19,20]. With specialized networking simulators, it is difficult to simultaneously consider various destabilizing disturbances during the simulation process. It is also complicated to take into account the transfer functions of networking equipment, which distort signals due to various inertial and nonlinear characteristics of the constituent blocks.

The general-purpose software package MatLAB / Simulink [21] allows to create a comprehensive model of the physical layer, including statistical characteristics of noises, transmission paths of radio signals etc. This approach lacks general analytical solutions when changing the channel parameters or signal propagation paths [22,23]. In [1] a hierarchical model for the physical level of FANET was developed, but no examples of modeling were presented.

2 Hierarchical signals generation model at the physical level

The hierarchical model of information signal generation should include multiple variants of communication channels and equipment for their analytical representation and analysis.

The generalized model should allow to describe communication channels in a flying network while taking into account attenuation, inter-symbol interference, and signal propagation over many paths. In addition, telecommunication equipment with linear and nonlinear signal conversion should be taken into account, and also circuits with different direction of control signals, namely direct control (FC), backward control (BC) and combined control, as well as multi-channel circuits.

The general scheme of the transformer of signals (TS) (Fig.1) contains similar TS, control unit (CU), control paths (CP) and weight distributor (WD). The generalized transformer consists of two control circuits: forward control (FC) and backward control (BC).

Each CP includes a series-connected detector (amplitude, frequency, or phase) and a filter. The CU controls the amplitude or phase of the signal. An administrative amplifier (attenuator), a controlled phase shifter, a voltage-controlled oscillator (VCO), etc. can be approximated by a control unit with a satisfying transmitting function. The values of the WD transmission coefficients allow the formation of the control and auxiliary output signals of the transformer. The blocks are designated as $TS_{x^2}^{x^1}$, where x^1 represents the level number, and x^2 the block number. Here U external basic input and output signals, u-auxiliary signals. The superscripts and subscripts of the signals are shown as $U_{y^2y^3}^{y^1}$, where superscript y^1 is the level number, the first subscript y^2 is the block number, and the second subscript y^3 is the signal identifier. The subscript y^3 might mean: 1-block input signal, 2-block output signal, U-control signal of the CU, f-CP of the FC circuit, b-CP of the BC circuit.

The TS scheme can be expanded similar to the TV raster by "rows" (expansion by levels) and by "frame". Fig. 1a and Fig. 1b show the second and α ($\alpha \geq 1$) levels of TS disclosure accordingly. The level α=0 corresponds to the unfolded (undisclosed) TS.

Let's designate the transfer functions of the blocks as follows: TS as Π, CU as K, WD as n, CP as W. As can be seen from Fig.1, the transfer functions of the TS at different levels are expressed as follows: level 0, $Q^0 = \Pi_1^0$-folded TS; level 1, $Q^1 = \Pi_1^1 K_1^1 \Pi_2^1$; level 2, $Q^2 = \Pi_1^2 K_1^2 \Pi_2^2 K_1^1 \Pi_3^2 K_2^2 \Pi_4^2$, etc. For level α

$$Q^{\alpha} = \Pi_{\beta}^{\alpha-1} = \Pi_{2\beta-1}^{\alpha} K_{\beta}^{\alpha} \Pi_{2\beta}^{\alpha}. \tag{2.1}$$

Taking into account the transfer functions of WD and CP for the current layer

$$\Pi_{\beta}^{\alpha-1} = \frac{U_{\beta}^{\alpha-1}{}_2}{U_{\beta}^{\alpha-1}{}_1} = \frac{\Pi_{2\beta}^{\alpha}\left(\Pi_{2\beta-1}^{\alpha} - f_{\beta_B}^{\alpha} K_{\beta_y}^{\alpha}\right)}{1 + \Pi_{2\beta}^{\alpha} f_{\beta_H}^{\alpha} K_{\beta_y}^{\alpha}} \tag{2.2}$$

where $f_{\beta_B}^{\alpha} = n_{\beta_B}^{\alpha} W_{2\beta-1}^{\alpha}$ and $f_{\beta_H}^{\alpha} = n_{\beta}^{\alpha} W_{2\beta}^{\alpha}$ transfer functions of the circuits FC and BC, respectively, $K_{\beta_y}^{\alpha}$ is the CU transfer function (for a signal $u_{\beta_y}^{\alpha}$).

Equating the right-wing part of expressions (2.1) and (2.2), we obtain the transfer function of the CU

$$\mathrm{K}_{\beta}^{\alpha} = \left({}_{2\beta-1}^{\alpha} - \mathrm{f}_{\beta\,2}^{\alpha} K_{\beta\,C}^{\alpha}\right) / \left({}_{2\beta-1}^{\alpha}(1 + {}_{2\beta}^{\alpha}\,\mathrm{f}_{\beta=}^{\alpha} K_{\beta\,C}^{\alpha})\right). \tag{2.3}$$

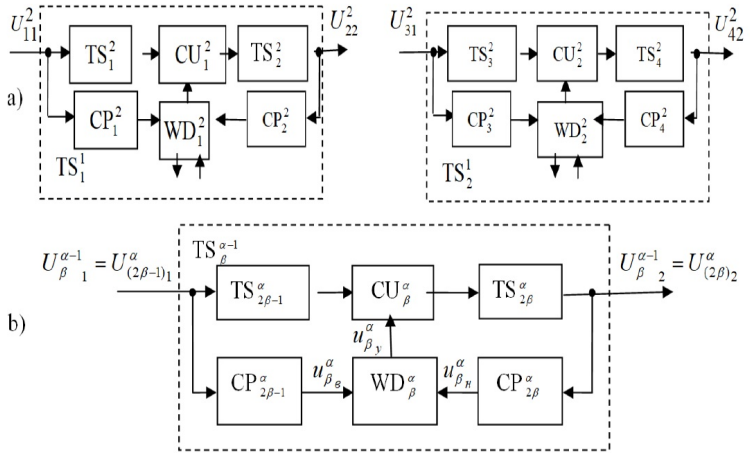

Figure 1: Hierarchical model of information signal generation at the physical level

If the forward and backward circuits are not present, the expression (2.3) might be simplified as following:

$$\Pi_{\beta}^{\alpha-1} = \Pi_{2\beta}^{\alpha}\Pi_{2\beta-1}^{\alpha}.$$

The proposed approach on the basis of signal transformer allows us to represent a particular FANET channel or a part of the networking equipment by the transfer functions in the corresponding fragment of the "frame" of the generalized hierarchical model [24-26].

3 Modeling of the UAV transmitter frequency synthesizer based on the hierarchical signal generation model

We approximate the scheme of a two-loop frequency-modulated digital frequency synthesizer (FM DFS) with frequency distortion compensation [27] (Fig. 2a) by the TS scheme (Fig. 2b). Two-loop tandem FM DFS are widely used in mobile radio communication systems as frequency-modulated band clock generators of transmitters [27-30]. The first loop of the pulse phase-locked loop (PLL1) generates an FM signal with a constant carrier frequency (about 80 MHz). This signal is used as a reference for the second loop of the pulse phase-locked loop (PLL2). It generates the output signal of the synthesizer in the range of higher frequencies (from 400 up to 800 MHz) with a specified step. Two-loop frequency synthesizers can successfully solve problems associated with an increase in the switching speed of operating frequencies, a decrease in phase noise near the carrier frequency, and a blockage of the frequency response in the upper modulating frequencies.

In Fig. 2, the following notation is used: CLK-clock quartz oscillator; PPM-pulse-phase modulator; DCamp-DC amplifier; Inv-inverter; DFD1, 2-frequency dividers with fixed division coefficients; DVD1-frequency divider with variable division coefficient; DFMD2-frequency divider with fractional-multiple variable division coefficient; FPD1, 2-frequency-phase detectors; Mod-modulating signal source; Att-controlled attenuator; Us1, Us2-amplifiers; VCO1, 2-voltage-controlled generators; LPF1, 2-low-pass filters. The numbers 1 and 2 indicate that the blocks belong to the first and second loop of the pulse phase-locked loop, respectively (PPL1 and PPL2).

We denote the parameters of the synthesizer circuit as follows: $K_A{=}R_2/N_2{=}R_2R/N$-transfer coefficient of attenuator; R_2 -coefficient of DFD2; $N_2{=}N/R$-DFMD2 division ratio, N and R are integers, N_1 -division ratio of DVD1; $S_{VCO1,2}$-slope coefficient of the VCO1 and VCO2 control characteristics; $F_1(p) = 1/[1 + pT_1)]$, $F_2(p) = 1/[1 + pT_2)]$-transfer function of LPF1 and LPF2, $T_{1,2}$-time constants of the filters; K_1 and K_2-gain of Amp1 and Amp2; S_{D1} and S_{D2}-detector characteristic slope coefficient of FPD1 and FPD2; $W_{AC}(p){=}1/[1{+}N_pF_1(p)]$-transfer function of an automatic compensator, $N_p{=}KS_{D1}S_M/R_1$– control coefficient, K is the gain of the DC amplifier, S_M-modulation characteristic slope of the PPM, R_1– division ratio of DFD1, u_M and U are the modulating and output signals of the synthesizer.

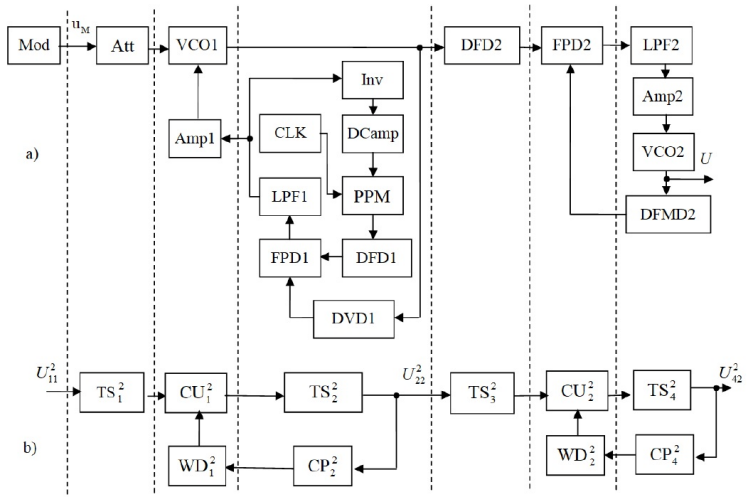

Figure 2: The scheme of a two-loop frequency-modulated digital frequency synthesizer (FM DFS) with frequency distortion compensation (a) represented by the TS scheme (b).

Then the transfer characteristics of the generalized scheme obtain the following form:

$$\Pi_1^2 = K_A S_{M1},\ K_{1_u}^2 = S_{M1},\ K_{2_u}^2 = S_{D2},\ n_1^2 = K_1,\ n_2^2 = \Pi_2^2 = 1$$
$$W_2^2 = \frac{2\pi}{pN_1} K_1 S_{D1} F_1(p) W_{AC}(p),\ \Pi_3^2 = \frac{2\pi}{pR_2},\ \Pi_4^2 = K_2 S_{M2} F_2(p),\ W_4^2 = \frac{2\pi R}{pN}. \tag{3.1}$$

The values of the remaining coefficients are zero. By substituting them into the final transfer functions of the generalized scheme we can obtain expressions for the amplitude and frequency modulation characteristics (AFMC), dynamic response of a specific synthesizer, etc. To approximate the scheme, one "line" and two levels of TS representation were required.

Based on (2.2), we obtain a generalized expression of the AFMC for a specific level of TS disclosure (Fig. 1b). We assume the following circuit blocks to be inertial: CP of the BC circuit (transfer function $W_{2\beta}^{\alpha}$) and both transformers ($\Pi_{2\beta-1}^{\alpha}, \Pi_{2\beta}^{\alpha}$). The transfer coefficients of the inertial blocks depend on the Laplace operator p.

We replace p with the complex frequency of the modulating signal $j\Omega$ and define the modulus of the formula (2.2). Then the expression of the AFMC takes the form

$$\left|\Pi_{\beta}^{\alpha-1}\right| = \sqrt{\frac{\left(\Pi_{2\beta-1_R}^{\alpha}\Pi_{2\beta_R}^{\alpha} - \Pi_{2\beta-1_I}^{\alpha}\Pi_{2\beta_I}^{\alpha} - n_{\beta_B}^{\alpha}K_{\beta_y}^{\alpha}W_{2\beta-1}^{\alpha}\right)^2 + \left(\Pi_{2\beta-1_R}^{\alpha}\Pi_{2\beta_I}^{\alpha} + \Pi_{2\beta-1_I}^{\alpha}\Pi_{2\beta_R}^{\alpha}\right)^2}{\left[1 + n_{\beta_H}^{\alpha}K_{\beta_y}^{\alpha}\left(\Pi_{2\beta_R}^{\alpha}W_{2\beta_R}^{\alpha} - \Pi_{2\beta_I}^{\alpha}W_{2\beta_I}^{\alpha}\right)\right]^2 + \left(n_{\beta_H}^{\alpha}K_{\beta_y}^{\alpha}\right)^2\left(\Pi_{2\beta_R}^{\alpha}W_{2\beta_R}^{\alpha} + \Pi_{2\beta_I}^{\alpha}W_{2\beta_I}^{\alpha}\right)^2}} \tag{3.2}$$

where $\Pi_R = \Pi_R(\Omega) = \mathrm{Re}[\Pi(j\Omega)]$ and $\Pi_I = \Pi_I(\Omega) = \mathrm{Im}[\Pi(j\Omega)]$.

Substituting the coefficients (3.1) in (3.2), we directly obtain the expressions for the AFMC of the FM DFS under research.

We find the coefficients taking into account the expression $W_{AC}(p)$. Since there are no general forward and backward connections, the transfer function of the converter takes the following form

$$\Pi_1^0 = \Pi_1^1\Pi_2^1,\ \Pi_1^1(p) = \frac{S_M \cdot R_2 \frac{R}{N}}{1 + \frac{1}{pT_1} \cdot F_1(p) \cdot \frac{1}{1+N_p F_1(p)}},\ \Pi_2^1(p) = \frac{\frac{N}{R} \cdot \frac{1}{R_2}}{1 + pT_2 \cdot \frac{1}{F_2(p)}}, \tag{3.3}$$

where $T_1 = N_1/2\pi S_{D1} S_{ry1} K_1$ and $T_2 = N_2/2\pi S_{D2} S_{M2} K_2$ are time constants of PLL1 and PLL2.

By substitution of p with $j\Omega$ in (3.3) we define the real and imaginary parts and substituting them into (3.2) we get the expressions of the normalized dimensionless AFMC of the PPL1 and PPL2

$$\left|\Pi_1^1(j2\pi F)\right| = 2\pi F T_1 \sqrt{\frac{(1+N_p)^2 + (2\pi F T_1)^2}{\left[1 - (2\pi F)^2 T_1 T_1\right]^2 + (2\pi F T_1)^2 (1+N_p)^2}}, \tag{3.4}$$

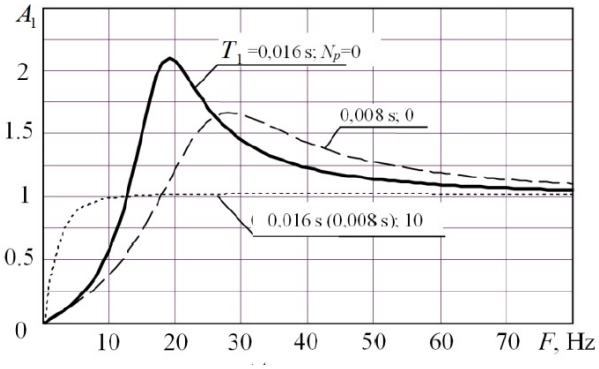

Figure 3: Modulation characteristics of the 1^{st} PLL for various time constants T_1 and regulation coefficients N_p.

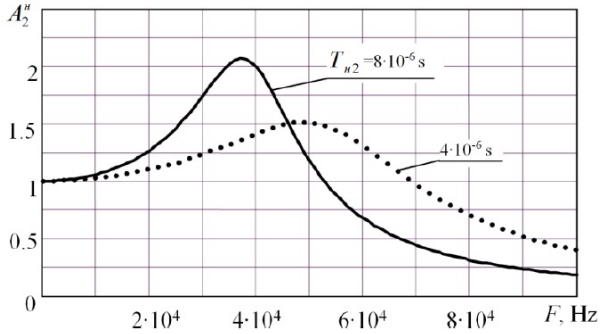

Figure 4: Modulation characteristics of the 2^{st} PLL for various time constants T_2.

$$\left|\Pi_2^1\left(j2\pi F\right)\right| = \frac{1}{\sqrt{\left[1-(2\pi F)^2 T_2 T_2\right]^2 + (2\pi F T_2)^2}}, \tag{3.5}$$

where $F = \Omega/2\pi$ is frequency of the modulating signal in Hz.

Expressions (3.4) and (**??**) coincide with those presented in [15], which confirms the correctness of the proposed method of analyzing devices based on TS. A change in the configuration of a particular synthesizer and the characteristics of its blocks is taken into account by simply changing the numerical coefficients in expression (3.2). Similarly, other characteristics, as well as the modes of the FM DFS, can be studied.

Fig. 3 shows the graphs $A_1(F)$ for various time constants T_1 and regulation coefficients N_p at $T_1 = 0.005s$ (the common value of the real FM DFS circuits). The time constants of the LPF1 correspond to the cutoff frequencies of 10 Hz and 20 Hz.

Fig. 4 shows the graphs for various at $A_2(F)$ for various T_2 at $T_2 = 2/10^{-6}$s. The LPF2 time constants correspond to the cutoff frequencies of 20 kHz and 40 kHz.

Analysis of the AFMC (Fig. 3) shows that in the absence of autocompensation, in order to reduce frequency distortion in the lower modulating frequency region, it is necessary to reduce the bandwidth of the LPF 1. In this case, it is obviously necessary to provide measures to ensure the specified performance. With the introduction of the autocompensator ($N_p = 10$), an AFMC form at lower modulating frequencies is almost independent on the LPF1 bandwidth (the maximum discrepancy of curves 1.3% is present at a frequency of 20 Hz) and is determined by the N_p coefficient. It allows to obtain a uniform AFMC in the lower modulating frequencies with increased LPF1 bandwidth.

The wide bandwidth of the LPF 2 (Fig. 4) ensures that the frequency response does not fall off in the region of the upper modulating frequencies when modulated by both analog and digital signals. So, at $T_2 = 4/10^{-6}$ s the descent of the AFMX begins only at F>68 KHz.

The conducted studies have confirmed the effectiveness of the use of autocompensators for the correction of AFMC and increasing the operating speed of two-loop FM DFS. The introduction of auto-compensation of frequency distortions makes it possible to linearize the frequency response in the low-frequency region while simultaneously expanding the bandwidth of the LPF ring PLL1, which increases the operating speed of the synthesizer. In the region of the

upper modulating frequencies, the autocompensator does not affect the decline of the AFMC and the distortion of the useful modulating signal.

If necessary, a set of sequentially connected blocks modeling signal propagation paths in the environment or receiver circuits might be added to the output of the model Fig. 1 or Fig. 2. This approach allows to represent a wide class of multi-channel network equipment. The developed analysis methodology can simplify the study of specific channels or networking equipment in networks of aircraft at the physical level.

4 Conclusion

Effective design of flying ad-hoc networks requires creating a reliable model of network behavior at various levels of OSI interaction. Specialized networking simulators are characterized by a simplified model of the physical layer. The influence of multiple heterogeneous factors (conditions of the ambient media, signal reflection conditions, various noises, inertia and non-linearity of communication equipment, etc. prevents simple creation of reliable network interaction models in the FANET at the physical level.

The developed hierarchical model allows to analytically describe diverse communication channels and networking equipment. Attenuation in the communication channel is considered by inertial frequency-dependent links. In order to take into account multipath propagation of signals, we might sum signals over individual paths (considering their time delays). Filters and nonlinear detectors allows the model to represent the linear and nonlinear network equipment. Forward control and backward control circuits allow to model the multi-channel signal generation and processing.

Modeling of the frequency synthesizer transmitter UAV based on a hierarchical signals generation model allowed us to explore the possibility of shaping a uniform amplitude-frequency modulation characteristics (AFMC) in the lower modulating frequencies of FM DFS with arbitrary bandwidth of the LPF in the first phase-locked loop, through the use of autocompensation methods of attenuation distortion. At the same time, the expansion of the LPF band allows to increase the operation speed of the first loop and the synthesizer as a whole.

Acknowledgment

The work was supported by the RFBR grant 19-29-06030-mk "Research and development of a wireless ad-hoc network technology between UAVs and smart city control centers based on the adaptation of transmission mode parameters at various levels of network interaction". The theory was prepared within the framework of the state task of the Russian Federation FZWG-2020-0029 "Development of theoretical foundations for building information and analytical support for telecommunications systems for geoecological monitoring of natural resources in agriculture".

References

[1] I.Y. Abualhaol and M.M. Matalgah, *Outage probability analysis in a cooperative UAVs network over nakagami-m fading channels*, IEEE Conf. Vehicular Technol., 2006, pp. 1–4.

[2] I.Y. Abualhaol and M.M. Matalgah, *Performance analysis of cooperative multi-carrier relay-based UAV networks over generalized fading channels*, Int. J. Commun. Syst. **24** (2011), no. 8, 1049–1064.

[3] A. Abdelrahman, H. Mohammad, A. Fayez, and A. Omar, *A Survey on Wireless Sensor Networks Simulation Tools and Testbeds*, Sensors, Transducers, Signal Conditioning and Wireless Sensors Networks Advances in Sensors, Vol. 3, Chapter 14, 2016.

[4] N. Ahmed, S. Kanhere, and S. Jha, *Link characterization for aerial wireless sensor networks*, GLOBECOM Wi-UAV Workshop, 2011, pp. 1274–127.

[5] G. Amos, *MATLAB: An Introduction with Applications: 2nd Edition*, John Wiley & Sons, 2004.

[6] S.L. Anisimov, *Tandem digital frequency synthesizers with a fractional-multiple frequency divider of the second ring*, Actual Issues Oper.f Secur. Syst. Protected Telecommun. Syst., 2007, pp. 8–9.

[7] S.L. Anisimov, E.A. Pechenin, and P.A. Popov, *Digital frequency synthesizer with frequency modulation, patent on utility model No. 62310 of the Russian Federation*, N03C 3/10, N 03L7/18, No. 2006143175/22, Declared on 07.12.2006, Published on 27.03.2007.

[8] S.L. Anisimov and P.A. Popov, *Construction of two-loop frequency-modulated frequency synthesizers on a modern digital element base*, Bull. Voronezh Inst. Ministry Internal Affairs Russia **1** (2007), 174–177.

[9] O. Bazan and M. Jaseemuddin, *On the design of opportunistic MAC protocols for multihop wireless networks with beamforming antennas*, IEEE Trans. Mobile Comput. 10 (2011), no. 3, 305–319.

[10] A. Cho, J. Kim, S. Lee, and C. Kee, *Wind estimation and airspeed calibration using a UAV with a single-antenna GPS receiver and pitot tube*, IEEE Trans. Aerospace Electronic Syst. **47** (2011), 109–117.

[11] E.P. de Freitas, T. Heimfarth, I.F. Netto, C.E. Lino, C.E. Pereira, A.M. Ferreira, F.R. Wagner, and T. Larsson, *UAV relay network to support WSN connectivity*, ICUMT, IEEE, 2010, pp. 309–314.

[12] Z. Huang and C.-C. Shen, *A comparison study of omnidirectional and directional MAC protocols for ad hoc networks*, Global Telecommun. Conf. (GLOBECOM), 2002.

[13] F. Jiang and A.L. Swindlehurst, *Dynamic UAV relay positioning for the ground-to-air uplink*, IEEE Globecom Workshops, 2010.

[14] E. Kuiper and S. Nadjm-Tehrani, *Mobility models for UAV group reconnaissance applications*, Proc. Int. Conf. Wireless Mobile Commun. (IEEE Computer Society), 2006.

[15] I.A. Kurilov and S.L. Anisimov, *Automatic compensation of frequency distortions in two-loop frequency-modulated digital frequency synthesizers*, Radio Engin. **9** (2008), 91–93.

[16] I. Maza, F. Caballero, J. Capitán, J.R. Martínez-De-Dios, and A. Ollero, *Experimental results in multi-UAV coordination for disaster management and civil security applications*, J. Intell. Robot. Syst. **61** (2011), no. 1-4, 563–585.

[17] G. Noubir, *On connectivity in ad hoc networks under jamming using directional antennas and mobility*, Wired/Wireless Internet Communications, Lecture Notes in Computer Science, vol. 2957, 2004, pp. 521–532.

[18] A. Qutaiba, *Simulation Framework of Wireless Sensor Network (WSN) Using MATLAB/SIMULINK Software, MATLAB*, A Fundamental Tool for Scientific Computing and Engineering Applications, Vol. 2, 2012.

[19] A. Qutaiba, A. Abdulmaowjod, and M. Hussein, *Simulation and performance study of wireless sensor network (WSN) using MATLAB*, 1st Int. Conf. Energy, Power Control (EPC-IQ), IEEE, 2010, pp. 307–314.

[20] R. Ramanathan, *On the performance of ad hoc networks with beamforming antennas*, Proc. 2nd ACM Int. Symp. Mobile Ad Hoc Network. Comput. (MobiHoc '01), 2001, pp. 95–105.

[21] E. Semsch, M. Jakob, D. Pavlícek, and M. Pechoucek, *Autonomous UAV Surveillance in Complex Urban Environments*, IEEE/WIC/ACM Int. Joint Conf. Web Intell. Intell. Agent Technol., Vol. 2. IEEE, 2009, pp. 82–85.

[22] Z. Sun, P. Wang, M.C. Vuran, M. Al-Rodhaan, A. Al-Dhelaan, and I.F. Akyildiz, *BorderSense: border patrol through advanced wireless sensor networks*, Ad Hoc Networks **9** (2011), no. 3, 468–477.

[23] V. Taliwal, D. Jiang, H. Mangold, C. Chen, and R. Sengupta, *Empirical determination of channel characteristics for DSRC vehicle-to-vehicle communication*, Proc. 1st ACM Int. Workshop Vehicular ad hoc Networks, 2004, pp. 88–88.

[24] G.S. Vasilyev, O.R. Kuzichkin, I.A. Kurilov, and D.I. Surzhik, *Development of methods to model UAVS nonlinear automatic control systems*, Rev. Univers. Zulia **11** (2020), no. 30, 137–147.

[25] G.S. Vasilyev, O.R. Kuzichkin, I.A. Kurilov, and D.I. Surzhik, *Development of a methodology to model the dynamic properties of UAVS and high-order control systems*, Rev. Univer. Zulia **11** (2020), no. 30, 189–199.

[26] G.S. Vasilyev, O.R. Kuzichkin, D.I. Surzhik, and I.A. Kurilov, *Algorithms for analysis of stability and dynamic characteristics of signal generators at the physical level in FANET networks*, Int. Conf. Comput. Sci. Commun. Network Secur. (CSCNS2019), December 22-23, 2019.

[27] G.S. Vasilyev, D.I. Surzhik, O.R. Kuzichkin, and K.V. Bondarik, *Hierarchical model of information signals formation at the physical layer in FANET*, 7th Int. Conf. Control Decis. Inf. Technol. (CoDIT'2020), June 29-July 2, 2020.

[28] W. Wang, X. Guan, B. Wang, and Y. Wang, *A novel mobility model based on semi-random circular movement in mobile ad hoc networks*, Inf. Sci. **180** (2010), no. 3, 399–413.

[29] H. Xiang and L. Tian, *Development of a low-cost agricultural remote sensing system based on an autonomous unmanned aerial vehicle*, Biosyst. Engin. **108** (2011), 174–190.

[30] J. Yin, G. Holl, T. Elbatt, F. Bai, and H. Krishnan, *DSRC channel fading analysis from empirical measurement*, Proc. 1st IEEE Int. Workshop on Vehicle Commun. Appl. (Vehiclecomm), 2006, pp. 25–27.